High-Throughput Screening

DOI: 10.1002/ange.200601302

Colloidal Crystal Beads as Supports for Biomolecular Screening**

*Xiangwei Zhao, Yun Cao, Fuyumi Ito, Hai-Hua Chen, Keiji Nagai, Yu-Hua Zhao, and Zhong-Ze Gu**

In high-throughput screening and multiplex analysis, a number of individual assays need to be carried out simultaneously within the same sample.[1] One approach is based on encoded carriers, on which probe biomolecules such as DNA strands or proteins are immobilized to bind the target molecules. When the carriers are encoded, they can be mixed and subjected to an assay simultaneously and then many binding events can be distinguished by their codes. The carriers may be spots on a microarray chip that are encoded by their coordinates. The advantage of this method is that the well-developed microfabrication technique can be utilized for chip fabrication. However, the probing speed needs to be improved because the molecular interaction on the chip is diffusion-limited.[2,3] The key is to immobilize biomolecules on encoded particles such as rods or beads, which can undergo free rotation and movement. These particles, known as fluidic carriers, have been drawing more and more attention.

Spectrum encoding is a well-used method of encoding because of its simplicity in detection and operation. Fluorescent dyes and quantum dots are the main spectrum-encoding elements.[4–7] These carriers, which are usually employed by the encoded fiber optics or Luminex system, are widely applied to genotyping, proteomics, and diagnostics.[7–10] However, the encoding elements tend to be quenched or bleached and their degree of multiplexing is limited because the optical spectra overlap. Recently, the reflection spectrum of a one-dimensional photonic crystal was proposed as a new encoding element.[11,12] The spectra come from the physical structure of the carriers, and therefore these codes are extremely stable compared with the organic or fluorescent

[*] X.-W. Zhao, Y. Cao, H.-H. Chen, Prof. Dr. Z.-Z. Gu
State Key Laboratory of Bioelectronics
Southeast University
Nanjing 210096 (China)
Fax: (+86) 25-8379-5635
E-mail: gu@seu.edu.cn
X.-W. Zhao, Prof. Y.-H. Zhao
College of Life Science
Zhejiang University
Hangzhou 310029 (China)
Dr. F. Ito, Dr. K. Nagai
Institute of Laser Engineering (ILE)
Osaka University
Osaka 565-0871 (Japan)

[**] This work was supported by the National Natural Science Foundation (grants 20573018 and 60121101).

Supporting information for this article is available on the WWW under http://www.angewandte.org or from the author.

dyes. However, it is inconvenient that 1D photonic crystal microcarriers have to be properly dispersed and correctly orientated to avoid stacking or standing of the flakes during the decoding process.[11] Recently, we found that these problems might be solved by microbeads with a three-dimensional photonic crystal structure.

One simple way to fabricate 3D photonic crystals is the assembly of monodisperse colloidal nanoparticles, which are also known as colloidal crystals.[13–19] Up to now, the main contribution was devoted to the fabrication of film, and there are only a few reports on the formation of spherical colloidal crystals.[15,17,20,21] Herein, we show an apparatus with which colloidal crystal beads of well-controlled size can be continuously fabricated. Figure 1 depicts the apparatus which was

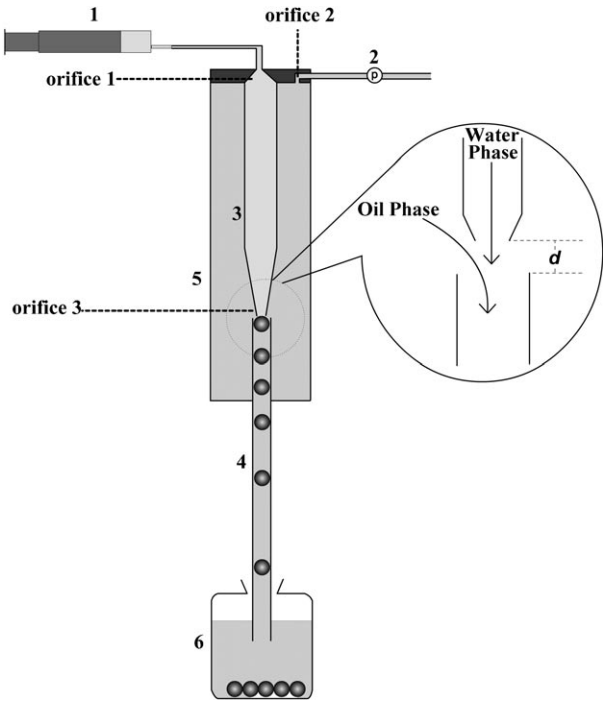

Figure 1. Diagram of the fabrication apparatus. 1) Syringe pump for aqueous suspension; 2) magnetic pump equipped with a flow meter for oil; 3) tapered glass tube; 4) glass tube; 5) cylinder; 6) collector. The magnified area in the circle shows the integration of orifice 3 and the glass tube 4.

originally developed for the fabrication of oil emulsions in water.[22,23] An aqueous-phase solution containing cross-linked monodisperse poly(methyl methacrylate) (PMMA) colloidal nanoparticles and an oil-phase solution are injected continuously into the droplet generator. Droplets of the aqueous solution are then generated on the tip of the tapered glass tube and flow into the collector. When the water in the droplets evaporates slowly, the monodisperse nanoparticles self-assemble into ordered lattices. The droplets are dried, and colloidal crystal beads are produced in which van der Waals forces hold the nanoparticles together.

The size of the colloidal crystal beads depends on both the concentration of nanoparticles and the size of the droplet. The beads enlarge when the concentration of particles in the droplet increases. Generally, the size of the droplets increases when the diameter of the tapered orifice, the extrusion rate of the water phase, or the distance *d* (see Figure 1) increases, and decreases when the velocity of the oil phase increases. Therefore, the size of the colloidal crystal beads can be well-controlled by manipulation of the above factors. Up to now, we have prepared colloidal crystal beads from tens of micrometers to several millimeters in diameter.

Figure 2 shows the reflection spectra of six kinds of colloidal crystal beads composed of monodisperse nanoparticles of different sizes. The reflection of the bead comes

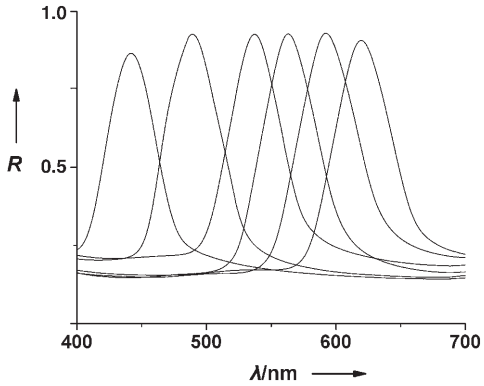

Figure 2. Reflection spectra of six colloidal crystal beads composed of PMMA nanoparticles with different sizes. From left to right, the sizes of the nanoparticles are 195, 208, 220, 230, 248, and 268 nm.

from the diffraction of light from the ordered structure (see Figure 3), which shifts to a long wavelength as the diameter of the nanoparticles increases. The reflection peak of one single bead is almost orientation-invariant, because the shift of the reflection peak at different positions is less than 5 nm. Hence, the orientation of the beads does not need to be considered during the decoding process.

Figure 3 shows scanning electron microscopy (SEM) images of a colloidal crystal bead. It can be observed that

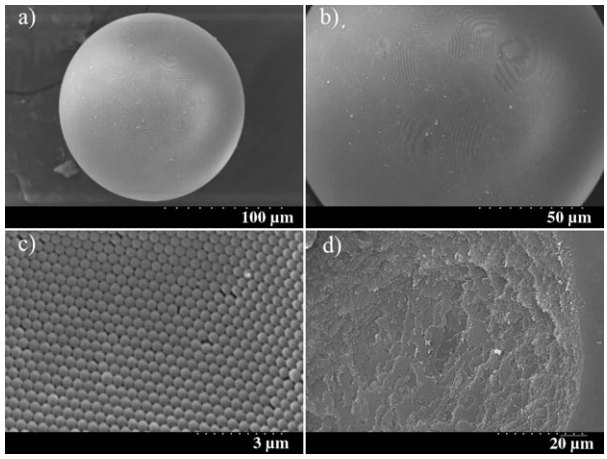

Figure 3. SEM images of the colloidal crystal beads. a) Low-magnification image of the colloidal crystal bead showing the smooth bead surface. b) Domains can be observed on the bead surface but no apparent cracks are visible. c) High-magnification image of the bead surface showing the hexagonal alignment of nanoparticles. d) Image of a split bead showing the inner structure.

the surface of the bead is smooth over a large area. Unlike the colloidal crystal film in which there are cracks every 10 to 50 μm, cracks are hardly observed in the colloidal crystal bead. The high-magnification image of the bead surface shows that the nanoparticles mainly form a hexagonal symmetry, which is the same in the colloidal crystal films. The cross section of a split bead shows that the nanoparticles also form an ordered structure inside the bead. All the beads fabricated by this method exhibit brilliant colors and sharp reflection peaks, which can be used as codes for carriers in high-throughput screening or multiplex bioassays. The codes of the beads can also be customized by varying the size of the nanoparticles according to Bragg's law. The reflection spectra of the beads, unlike those of fluorescent dyes, are very stable to light irradiation and long-term storage. No apparent spectral change was detected after several months of storage at room temperature.

To demonstrate the reliability of the colloidal crystal beads as encoded carriers in a multiplex bioassay, we prepared three kinds of beads composed of 250-, 220-, and 210-nm cross-linked PMMA nanoparticles, which were red, green, and blue, respectively (Figure 4). Human, mouse, and rabbit immunoglobulin G (IgG) were physically absorbed onto the red, green, and blue colloidal crystal beads, respectively, by overnight incubation at 4 °C. The sites on the bead surfaces that did not absorb protein were blocked with a solution of bovine serum albumin (BSA). The three kinds of beads were mixed and exposed to a solution containing fluorescein isothiocyanate (FITC)-conjugated goat anti-human and anti-rabbit IgG. After incubation and rinsing, the fluorescence and reflection spectra were measured using a microscope equipped with a fiber optics spectrometer (Figure 4). Fluorescence was detected on the red and green beads at 520 nm, while no fluorescence signal was detected on the blue beads. The result indicated that human and mouse IgG on red and green beads bond specifically with goat anti-human and anti-mouse IgG tagged with FITC. This finding is consistent with the content of the sample to which the beads were exposed.

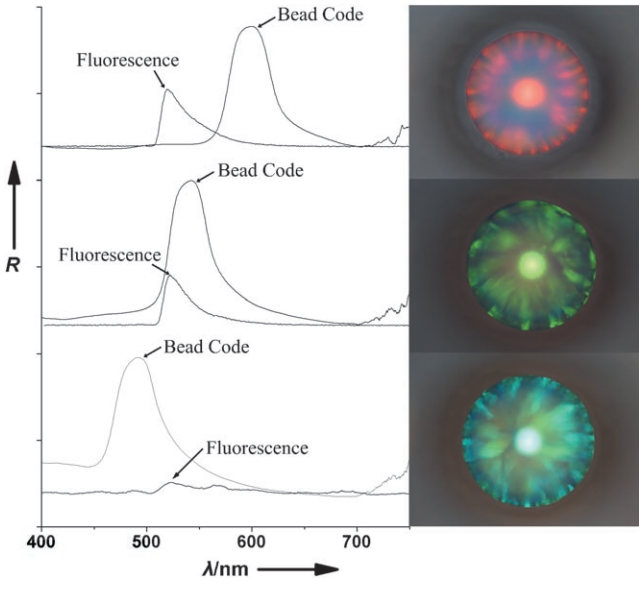

Figure 4. Fluorescence and optical reflection spectra (left) and bright-field microscopic images (right) of three colloidal crystal beads with a diameter of 400 μm. The red, green, and blue beads were immobilized with human, mouse, and rabbit IgG, respectively. They were exposed to a sample containing FITC-tagged goat anti-human IgG and goat anti-rabbit IgG. Both the fluorescence and reflection measurements were performed on an Olympus fluorescence microscope with a 10× objective coupled to an Ocean Optics spectrofluorometer (USB2000-FLG). Spectra are offset along the *R* axis for clarity.

In summary, we have developed an approach for fabricating colloidal crystal beads of controllable size and demonstrated their use in multiplex bioassays. This approach has the following advantages over the reported methods. 1) The beads are fabricated continuously. Both the apparatus and fabrication process are suitable for mass production. 2) The reflection peak of the colloidal crystal bead is both sharp and orientation-invariant. No orientation is needed for the optical decoding. In addition, the fabrication method can be extended to core–shell beads, in which core and shell are composed of nanoparticles of different sizes. In this case, the colloidal crystal beads are encoded by two or more reflection peaks, which can greatly increase the encoding capacity. 3) As the colloidal crystal beads are assemblies of nanoparticles, the surface functional groups such as NH_2 and COOH or surface wettability can be customized by selecting appropriate nanoparticles. 4) As they are composed of hexagonal close-packed nanoparticles, the bead surfaces are coarse in the submicrometer scale, which increases the surface-to-volume ratio and thus the detection sensitivity. 5) Compared with the optical absorption encoded carriers, the code generated by photonic crystals is very stable to light irradiation and long-term storage. In addition to the reflective features of photonic crystals, the fluorescence absorption from the surface fluorescent dyes can be reduced and as a result the fluorescence intensity and the sensitivity are enhanced.[24] Therefore, wide applications of colloidal crystal beads are anticipated in genomic or proteomic studies, drug screening, clinical diagnostics, and combinatorial chemistry.

Received: April 3, 2006
Revised: August 5, 2006
Published online: September 26, 2006

Keywords: colloids · high-throughput screening · immunoassays · nanoparticles · self-assembly

[1] K. Braeckmans, S. De Smedt, M. Leblans, R. Pauwels, J. Demeester, *Nat. Rev. Drug Discovery* **2002**, *1*, 447.
[2] S. R. Nicewarner-Pena, R. G. Freeman, B. D. Reiss, L. He, D. J. Pena, I. D. Walton, R. Cromer, C. D. Keating, M. J. Natan, *Science* **2001**, *294*, 137.
[3] M. R. Henry, P. W. Stevens, J. Sun, D. M. Kelso, *Anal. Biochem.* **1999**, *276*, 204.
[4] M. Trau, B. J. Battersby, *Adv. Mater.* **2001**, *13*, 975.
[5] R. J. Fulton, R. L. McDade, P. L. Smith, L. J. Kienker, J. John, R. Kettman, *Clin. Chem.* **1997**, *43*, 1749.
[6] M. Han, X. Gao, J. Su, S. Nie, *Nat. Biotechnol.* **2001**, *19*, 631.
[7] F. Steemers, J. Ferguson, D. Walt, *Nat. Biotechnol.* **2000**, *18*, 91.
[8] F. Szurdoki, K. L. Michael, D. R. Walt, *Anal. Biochem.* **2001**, *291*, 219.

[9] J. Ferguson, F. Steemers, D. Walt, *Anal. Chem.* **2000**, *72*, 5618.
[10] www.luminexcorp.com.
[11] F. Cunin, T. Schmedake, J. Link, Y. Li, J. Koh, S. Bhatia, M. Sailor, *Nat. Mater.* **2002**, *1*, 39.
[12] J. Y. Kim, F. E. Osterloh, *J. Am. Chem. Soc.* **2006**, *128*, 3868.
[13] O. D. Velev, K. Nagayama, *Langmuir* **1997**, *13*, 1856.
[14] A. Imhof, D. J. Pine, *Nature* **1997**, *389*, 948.
[15] G. R. Yi, J. H. Moon, S. M. Yang, *Adv. Mater.* **2001**, *13*, 1185.
[16] G. R. Yi, V. N. Manoharan, S. Klein, K. R. Brzezinska, D. J. Pine, F. F. Lange, S. M. Yang, *Adv. Mater.* **2002**, *14*, 1137.
[17] J. H. Moon, G. R. Yi, S. M. Yang, D. J. Pine, S. Bin Park, *Adv. Mater.* **2004**, *16*, 605.
[18] Z. Z. Gu, Y. H. Yu, H. Zhang, H. Chen, Z. Lu, A. Fujishima, O. Sato, *Appl. Phys. A* **2005**, *81*, 47.
[19] G. R. Yi, J. H. Moon, V. N. Manoharan, D. J. Pine, S. M. Yang, *J. Am. Chem. Soc.* **2002**, *124*, 13354.
[20] Z. Z. Gu, A. Fujishima, O. Sato, *Chem. Mater.* **2002**, *14*, 760.
[21] P. Jiang, J. F. Bertone, K. S. Hwang, V. L. Colvin, *Chem. Mater.* **1999**, *11*, 2132.
[22] H. Yang, K. Nagai, X. Zhao, H. Chen, Z.-Z. Gu, *J. Nanosci. Nanotechnol.* **2005**, *5*, 1821.
[23] K. Nagai, M. Nakajima, T. Norimatsu, Y. Izawa, T. Yamanaka, *J. Polym. Sci. Part A* **2000**, *38*, 3412.
[24] P. Vukusic, I. Hooper, *Science* **2005**, *310*, 1151.

